Topological superconductivity in a magnetic-texture coupled Josephson junction

Ignacio Sardinero [1,2] Rubén Seoane Souto [3,4,5] and Pablo Burset [1,2,6]

[1]*Department of Theoretical Condensed Matter Physics, Universidad Autónoma de Madrid, 28049 Madrid, Spain*

[2]*Condensed Matter Physics Center (IFIMAC), Universidad Autónoma de Madrid, 28049 Madrid, Spain*

[3]*Division of Solid State Physics and NanoLund, Lund University, S-221 00 Lund, Sweden*

[4]*Center for Quantum Devices, Niels Bohr Institute, University of Copenhagen, DK-2100 Copenhagen, Denmark*

[5]*Instituto de Ciencia de Materiales de Madrid (ICMM), Consejo Superior de Investigaciones Científicas (CSIC), Sor Juana Inés de la Cruz 3, 28049 Madrid, Spain*

[6]*Instituto Nicolás Cabrera, Universidad Autónoma de Madrid, 28049 Madrid, Spain*

Topological superconductors are appealing building blocks for robust and reliable quantum information processing. Most platforms for engineering topological superconductivity rely on a combination of superconductors, materials with intrinsic strong spin-orbit coupling, and external magnetic fields, detrimental for superconductivity. We propose a setup where a conventional Josephson junction is linked via a magnetic-textured barrier. Antiferromagnetic and ferromagnetic insulators with periodically arranged domains are compatible with our proposal, which does not require intrinsic spin-orbit or external magnetic fields. We find that the topological phase depends on the magnitude and period of the barrier magnetization. The superconducting phase controls the topological transition, which could be detected as a sharp suppression of the supercurrent across the junction.

Introduction. Majorana bound states (MBSs) are charge neutral, zero-energy quasiparticle excitations appearing at the boundaries of topological superconductors [1–6]. A pair of MBSs localized at the ends of a one-dimensional (1D) topological superconductor encodes a nonlocal fermionic state [7]. These states are robust against local perturbations and display non-Abelian exchange properties [8,9], making them attractive for fault-tolerant quantum information processing [10]. The experimental realization of topological MBSs requires the combination of superconductivity, helical electrons usually created from spin-orbit coupling, and time-reversal breaking from magnetism [11]. Over the last decade [12], several material platforms have been explored based on topological insulators [13,14], semiconductor nanowires [5,15–17], planar Josephson junctions [18–24], chains of magnetic adatoms [25–27], and, recently, ferromagnetic insulators combined with other time-reversal symmetry breaking effects [28–41].

An alternative strategy has been recently implemented where the spin orbit is synthetically engineered using spatially varying magnetic fields [42–46]. In proximitized one-dimensional (1D) systems, the spatial magnetic modulation can be achieved by interactions [47–49], adatoms [50–59], or local magnets [60–64]. Planar setups offer more sophisticated magnetic textures in proximity to superconductors [65–79]. For example, skyrmion textures on superconductors [80–83] have been recently measured [84,85] and signatures consistent with MBSs where found in proximitized magnetic monolayers [86–88]. Proximitized structures need to be carefully engineered so that the competing magnetic and superconducting orders coexist. This challenge could be circumvented if the magnetic texture featuring synthetic spin-orbit interaction is coupled to superconducting contacts in a Josephson

setup [42]. Magnetic textures with spatial variation across the junction, i.e., from contact to contact [44], have been implemented [42]. However, for future braiding applications a higher degree of control over the emerging MBSs could be achieved with textures along the junction interface, see Fig. 1.

Here, we explore such a configuration studying the topological properties of a two-dimensional (2D) Josephson junction (JJ) coupled through a magnetic-textured barrier [Fig. 1(a)] with a spatial modulation along the junction interface [Fig. 1(b)]. We find that the system enters the topological phase when the superconducting coherence length and the magnetization periodicity are comparable. The topological regime, characterized by MBSs localized at the edges of the JJ [Fig. 1(c)], can extend up to rather large occupations and is very sensitive to the phase bias across the junction. Moreover, we show that the formation and localization of pairs of MBSs has an observable effect on the junction current-phase relation. The superconducting phase difference is a substitute of
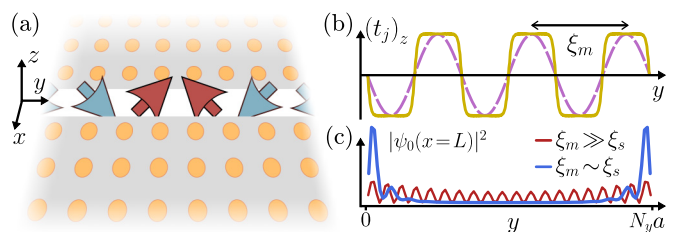

FIG. 1. Josephson junction mediated by a magnetic-textured barrier. (a) Two superconductors are linked by a magnetic-texture barrier with a local magnetization that changes in space, schematically represented by arrows. (b) Two possible magnetic texture profiles. (c) Localization of the ground state wave function at the interface in the trivial (red) and topological (blue) regimes.

the external magnetic field and helps reaching the topological regime [18,19,89]. Recent experiments have already shown the possibility of tuning subgap states varying the phase difference between planar Josephson junctions [20,21,37,90–92]. Our proposal is thus highly controllable, does not require external magnetic fields, and bypasses the need for intrinsic spin-orbit coupling and low-carrier densities.

Model and formalism. We consider a JJ formed by two conventional singlet *s*-wave superconductors joined by a magnetic-textured barrier, see Fig. 1. We model the system using a square-lattice tight-binding Hamiltonian $H = H_L + H_R + H_t$, with

$$
H_{\text{L,R}} = \sum_{\sigma=\uparrow,\downarrow} \left(-t \sum_{\langle x,x'\rangle} c_{i'j',\sigma}^\dagger c_{ij,\sigma} - \sum_{i,j} \mu_{ij} c_{ij,\sigma}^\dagger c_{ij,\sigma} \right)
$$
$$
+ \sum_{i,j} \Delta_0 e^{i\phi_{\text{L,R}}} c_{ij,\uparrow}^\dagger c_{ij,\downarrow}^\dagger + \text{H.c.}, \tag{1}
$$

being the Hamiltonian of the superconducting leads, where $\langle x, x'\rangle$ stands for nearest-neighbors combinations of the horizontal and vertical indices i, i' and j, j'. The operator $\hat{c}_{ij,\sigma}^\dagger$ ($\hat{c}_{ij,\sigma}$) creates (annihilates) an electron with spin σ on the lattice site (i, j). Here, t is the nearest-neighbors hopping integral, $\mu_{ij} \equiv \mu$ the uniform chemical potential of the lattice, $\Delta_0 > 0$ the superconducting pairing amplitude, and $\phi_{\text{L,R}}$ the superconducting phases; we denote their phase difference as $\phi = \phi_R - \phi_L$. We consider a finite-size lattice with N_x and N_y horizontal and vertical sites, respectively, and only examine symmetric junctions where both superconductors have the same gap, length $L = N_x a/2$ (with a being the lattice distance constant), and width $N_y a$.

The superconductors couple via a magnetic-textured barrier mediating tunneling between them,

$$
H_t = -\frac{1}{2} \sum_{\sigma,\sigma'} \sum_j t_{j,\sigma\sigma'} \hat{c}_{L,j,\sigma}^\dagger \hat{c}_{L+1,j,\sigma'} + \text{H.c.} \tag{2}
$$

We consider that the magnetization of the barrier has a spatial modulation, given by the matrix in spin space

$$
\hat{t}_j = t_0 \hat{\sigma}_0 + \boldsymbol{t}_j \cdot \boldsymbol{\sigma}. \tag{3}
$$

The index j runs along the width of the junction (Fig. 1) and $\boldsymbol{\sigma}$ is the vector of Pauli matrices $\hat{\sigma}_{0,1,2,3}$ in spin space. Here, t_0 is the uniform amplitude for the spin-conserving hopping term and $\boldsymbol{t}_j$ the spatially varying spin-tunneling part.

Analytic 1D topological model. To study the bulk topological properties of the system, we consider a perfect harmonic spatial variation along the spin yz plane with period ξ_m and constant magnitude t_{m},

$$
\boldsymbol{t}_j = t_m[0, \sin(2\pi ja/\xi_m), \cos(2\pi ja/\xi_m)]. \tag{4}
$$

We reach a solvable model setting $N_x = 2$, effectively reducing the system to two superconducting linear chains coupled along the y direction by Eq. (4), and assuming $N_y \to \infty$, i.e., applying periodic boundary conditions to go to the bulk limit. Then, we change into a rotating-frame basis so that the magnetization orientation always falls along the z axis [60]. As a result, the two linear superconductors acquire an effective spin-orbit coupling [47,60,61,93], and are described by the

(left, right) Hamiltonians

$$
\hat{h}_{\text{L,R}} = \left(-2t\cos(k_y a) - \mu - \frac{\pi^2}{\xi_m^2} \right) \hat{\sigma}_0 \hat{\tau}_3
$$
$$
+ \sin(k_y a)\frac{2\pi i}{\xi_m} \hat{\sigma}_2 \hat{\tau}_3 + \Delta_0 e^{i\phi_{\text{L,R}}} \hat{\sigma}_2 \hat{\tau}_2, \tag{5}
$$

coupled by the tunnel Hamiltonian

$$
\hat{h}_t = (t_0 \hat{\sigma}_0 + t_m \hat{\sigma}_3) e^{i\phi/2} \hat{\tau}_3, \tag{6}
$$

with $\hat{\tau}_{1,2,3}$ acting in Nambu (particle-hole) space.

The Hamiltonian of each linear chain $\hat{h}_{\text{L,R}}$ is particle-hole and mirror symmetric, while $\hat{h}_t$ breaks time-reversal symmetry. Therefore, the system is in BDI class [18,94] and can be characterized by a $\mathcal{W} \in \mathbb{Z}$ invariant [95], whose parity $\mathcal{M} = (-1)^{\mathcal{W}} \in \mathbb{Z}_2$ can be determined after a change to the so-called Majorana basis. Rewriting $H(k_y) = \hat{h}_L + \hat{h}_R + \hat{h}_t$ as a skew-symmetric matrix A is possible by a unitary transformation, and we thus reach

$$
\mathcal{M} = \text{sgn}\{\text{Pf}[A(0)]/\text{Pf}[A(\pi/a)]\}, \tag{7}
$$

with Pf$[A]$ referring to the Pfaffian of A. See Supplemental Material (SM) [96] for more details.

Topological superconductivity. Using the analytic model as a guide, we now focus on the finite-size system depicted in Fig. 1 and described by Eqs. (1) and (2). We first consider a harmonic variation of the magnetic texture with constant amplitude t_m, Eq. (4), although our findings remain qualitatively invariant for other periodic magnetization profiles [96]. The barrier locally polarizes the tunneling electrons inducing an effective exchange field in the two superconductors. Additionally, we account for a local exchange field close to the barrier [96].

In the absence of magnetism ($t_m = 0$), the system features a set of spin-degenerate Andreev bound states inside the superconducting gap with an energy that depends on the phase and the transmission of the channel [97]. A uniform spin polarization along a fixed direction, $\boldsymbol{t}_j = t_m(0, 0, 1)$, splits these subgap states in two different spin species, eventually closing the superconducting gap. The system, however, is still in the trivial phase. We describe the magnetic texture by introducing the spatial variation in Eq. (4), which mixes the two spin components facilitating the formation of equal-spin triplet pairing close to the junction [98], to the second term of Eq. (3). We now describe the conditions for the gap reopening indicating a transition into the topological phase with localized MBSs at the edges of the JJ.

To characterize the topological phase of the finite system we define an approximate topological invariant $\bar{\mathcal{W}}$, which we compute as the number of MBSs pairs lying at $E \approx 0$ separated from the subsequent bulk modes by an effective gap $\delta \leqslant \Delta_0$ [96]. The system features two Majorana states ($\bar{\mathcal{W}} = 1$) when the chemical potential of the 2D superconductors is $\mu \sim -3.5t$. This regime is shown in Fig. 2(a) highlighted by a blue background color. Other topological phases with $\bar{\mathcal{W}} > 1$ appear at higher fillings of the superconductors, shown as a yellow background in Fig. 2(a). We thus focus below on fillings with only one MBS pair.

We compute $\bar{\mathcal{Q}} = (-1)^{\bar{\mathcal{W}}}\delta/\Delta_0$ in Figs. 2(b)–2(d) to characterize the topological phase and show that the magnetic
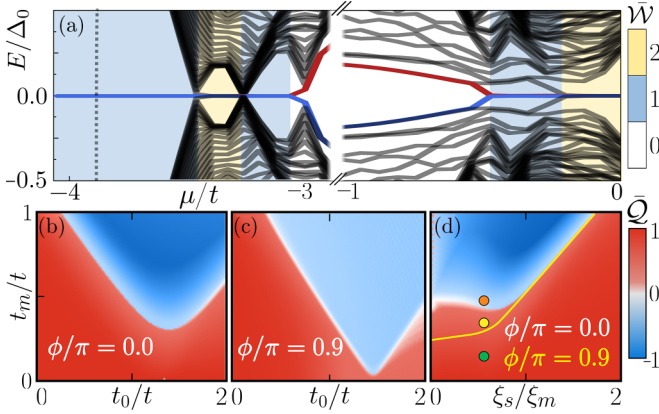
FIG. 2. Topological phase diagram. (a) Lowest 40 energy bands as a function of the chemical potential for $\xi_m \approx 0.8\xi_s$ and $t_m/t = 0.75$. The colored background represents the number of pairs of edge states $\bar{\mathcal{W}}$. (b)–(d) show maps of $\bar{\mathcal{Q}}$ at $\mu/t = -3.8$; blue indicates the topologically nontrivial phase. (b), (c) $\bar{\mathcal{Q}}$ with $\xi_m = \xi_s$ as a function of t_0 and t_m for (b) $\phi = 0$ and (c) 0.9π. (d) $\bar{\mathcal{Q}}$ as a function of t_m and ξ_m for $t_0/t = 1$ and $\phi = 0$. The topological phase boundary for 0.9π is highlighted as a yellow line. In all cases, $\Delta_0/t = 0.2$ and $N_x \times N_y = 16 \times 128$.

tunneling t_m required to enter the topological regime (blue regions) is minimal close to $t \approx t_0$, where the junction's normal transmission is maximal. In the analytic 1D model, the boundary between topological phases for $\phi = 0$ [white regions in Figs. 2(b)–2(d)] follows the simple condition [96]

$$t_m^2 = [\mu_{\text{eff}}(\xi_m) \pm t_0]^2 + \Delta_0^2, \qquad (8)$$

with $\mu_{\text{eff}}(\xi_m) = 2t - \mu + \pi^2/\xi_m^2$ [96]. The topological phase appears when $|\mu_{\text{eff}}| = t_0$ and $t_m = \Delta_0$. These parameters represent a junction with finite but not dominant reflections for both spin channels; a rather generic occurrence. The corresponding minimum of the nontrivial phase qualitatively coincides with that of the blue region of Fig. 2(b).

The phase difference ϕ between superconductors provides another way of controlling the topological phase transition. Tuning ϕ from 0 to π reduces the energy of the subgap states so that the phase transition occurs for lower t_m values, with a minimum located at $\phi = \pi$ (mod 2π). Figure 2(c) shows the phase diagram for $\phi = 0.9\pi$ illustrating the reduction of the minimal t_m required to enter the topological phase with respect to the $\phi = 0$ case shown in Fig. 2(b). However, we note that now the topological gaps are smaller (lighter blue in the topological region) than the ones found for $\phi = 0$. From the 1D model, the minimal required t_m value is given by

$$t_m^{\text{min}} = \Delta_0 \sqrt{1 + \cos\phi + \Delta_0^2 \frac{\sin^2\phi}{2\mu_{\text{eff}}(\xi_m)}}, \qquad (9)$$

with the limits $t_m(\phi = 0) = \Delta_0$ and $t_m(\phi = \pi) = 0$ [96]. Comparing the minima in Fig. 2(b) and Fig. 2(c) shows that these results are in qualitative agreement with the finite-size calculations.

The spatial periodicity of the magnetic texture, ξ_m, is another important parameter for reaching the topological phases, see Fig. 2(d). The local magnetization induced in the superconductors decays with a typical length scale given by the
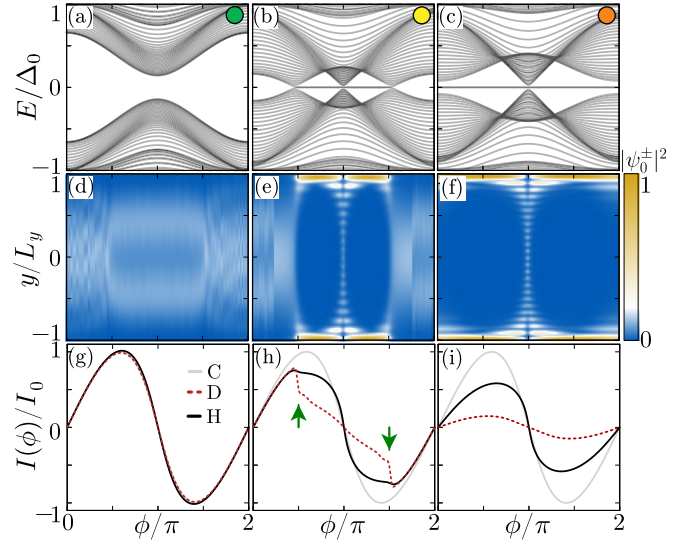

FIG. 3. Phase-controllable topological order. (a)–(c) Phase dependence of energy bands for $t_m/\Delta_0 = 1.0, 2.0$, and 2.5 in the barrier with harmonic texture. (d)–(f) Spatial distribution of the lowest-energy wave function $|\psi_0^{\pm}|^2$ evaluated along the junction interface ($i = L$). (g)–(i) Current-phase relation in the case of the clean (C), harmonic (H), and domain-textured (D) junctions. I_0 is the current maximum for the clean junction with $t_m = 0$ and $t_0 = t$. Arrows indicate the kink at the phase transition. In all cases, $\mu/t = -3.8$, $\xi_m = 2\xi_s$, and $\Delta_0/t = 0.2$.

superconducting coherence length ξ_s [99]. Therefore, for long magnetic periods, $\xi_s/\xi_m \ll 1$, electrons only feel the exchange field locally induced by the barrier and the gap collapses for sufficiently strong t_m values. In the opposite regime of small magnetic periods, $\xi_s/\xi_m \gg 1$, the barrier magnetization cannot close the superconducting gap and the system remains in the trivial phase. Consequently, a robust topological phase requires $\xi_s/\xi_m \sim 1$ where the topological gap is maximum while the t_m required for the phase transition is minimal [Fig. 2(d)].

Phase-controlled topological order. We now discuss in more detail the effect of the phase difference between superconductors. As shown in Fig. 2, the system can transition from the trivial to the topological regime when increasing the phase difference. Therefore, a finite superconducting phase difference reduces the energy of the subgap states, making it possible to transition to the topological regime for smaller t_m values. The superconducting phase is thus a convenient parameter to control topology and, consequently, the emergence and localization of MBSs. As an illustration, we compare in Fig. 3 three different configurations: far into the trivial region (left column); close to the boundary between topological phases from the trivial region (center); and inside the nontrivial phase (right column). In the first case (left), the modulation of the subgap states with the phase is insufficient to close the gap. The center column shows a gap closure and reopening for a finite phase ($\phi \sim \pi/2$), so that a pair of topological edge states appear when it reopens ($\phi > \pi/2$). Figures 3(d)–3(f) display the ground-state wave functions, $|\psi_0^{\pm}|^2$, showing the formation of localized edge modes in the topological regime. In the nontrivial case (right column), the superconducting phase increases the topological gap in the region away from

$\phi = 0$ and $\phi = \pi$. At $\phi = \pi$ the gap collapses and Majoranas delocalize across the full system.

The results presented thus far correspond to a harmonically rotating magnetic texture along the junction interface [dashed line in Fig. 1(b)]. A more realistic texture is represented by the solid line in Fig. 1(b) featuring anti-parallel domains with noncoplanar domain walls described by

$$\boldsymbol{t}_j = t_m \lambda_0^{-1}[0, \tanh(\lambda \sin y_j), \tanh(\lambda \cos y_j)], \qquad (10)$$

with $y_j = 2\pi ja/\xi_m$, $\lambda_0 = \tanh(\lambda)$ and the parameter λ controlling the length of the magnetic domains [96]. Using this domain magnetization model with the same parameters of Fig. 2 we reproduce the positions of the crossings in Fig. 3 and the overall structure of the map is preserved, see Ref. [96]. Consequently, we conclude that the details of the magnetic texture do not qualitatively affect the topological phase, as long as $\xi_s/\xi_m \sim 1$.

Finally, we compute the Josephson current at zero temperature, i.e., $I \propto \sum_{\epsilon_i<0} \partial_\phi \epsilon_i(\phi)$, for the negative eigenvalues ϵ_i of the full Hamiltonian [96]. We show the current-phase relation (CPR) for the three cases commented above in Figs. 3(g)–3(i). Interestingly, the phase-induced topological transition as a function of the phase appears as a kink on the CPR, see arrows in Fig. 3(h). This kink is produced by an avoided crossing of the remaining trivial Andreev bound states resulting from the topological protection of the newly formed gap, and it is more pronounced for the domain texture (red dashed lines) than for the harmonic case.

Role of the magnetization profile. The domain-texture model, Eq. (10), allows us to systematically introduce disorder by randomizing the domain size (ξ_m), domain magnetization (t_m), or domain wall helicity. Weak disorder in ξ_m and t_m does not disrupt the topological phase because these quantities preserve the system symmetry [96]. Indeed, disorder on ξ_m makes the topological gap size variable along the interface, since it is controlled by the magnitude of the effective spin-orbit coupling; while random domain magnetization values broaden the value of ϕ needed for the phase transition, thus making the avoided crossing in Fig. 3 wider and the kink less pronounced. Conversely, changes in domain wall helicity alter the sign of the effective spin-orbit coupling along the wire, leading to topological phase boundaries where different highly overlapping subgap modes can enter the topological gap [96].

Experimental implementation. Our proposal requires magnetic textures that have a characteristic length that is comparable to the superconducting coherence length. Recent experiments [100–103] reported magnetic textures with periodicity ranging from a few to hundreds of nm. These lengths are comparable to the characteristic coherence length of a

variety of superconductors [104,105]. Thin barriers, including atomically thin van der Waals materials [101,102] or few-atom layers [106] could be used to facilitate the Josephson effect in the setup we consider (Fig. 1). Moreover, in some cases the orientation of the magnetic texture can be tuned by external parameters to avoid stray fields across the junction [102,107]. Our proposal is thus within experimental reach after Josephson junctions with similar characteristics have been implemented [108–112].

Conclusions. In this work, we have shown the onset of topological superconductivity in a Josephson junction mediated by a spin-textured barrier. Using a two-dimensional tight-binding model, we identified the conditions for the emergence of topological Majorana zero modes at the edges of the system. The presence of the magnetic texture eliminates the need for spin-orbit coupling or external magnetic fields, while the phase bias across the junction provides control over the topological phase. We support these results computing the topological invariant in an analytical 1D model of the junction. Additionally, we investigate the impact of disorder on the topological phase transition, finding that only sign changes of the magnetic texture's helicity introduce trivial states within the topological gap.

Our work proposes a platform for topological superconductors that do not rely on intrinsic spin-orbit coupling and external magnetic fields. Materials including antiferromagnetic insulators with a small out-of-plane magnetization or ferromagnetic insulators with ordered domains are suitable candidates for magnetic-textured barriers [113–119]. The possible detrimental effect from stray fields could be reduced by choosing a texture with fields pointing away from the superconductors. Moreover, a geometrical modulation of the magnetic texture could improve the localization of the Majorana edge states [22,23].

[1] M. Leijnse and K. Flensberg, Introduction to topological superconductivity and Majorana fermions, Semicond. Sci. Technol. **27**, 124003 (2012).

[2] J. Alicea, New directions in the pursuit of Majorana fermions in solid state systems, Rep. Prog. Phys. **75**, 076501 (2012).

[3] R. Aguado, Majorana quasiparticles in condensed matter, La Rivista del Nuovo Cimento **40**, 523 (2017).

[4] R. M. Lutchyn, E. P. A. M. Bakkers, L. P. Kouwenhoven, P. Krogstrup, C. M. Marcus, and Y. Oreg, Majorana zero modes in superconductor–semiconductor heterostructures, Nat. Rev. Mater. **3**, 52 (2018).

[5] E. Prada, P. San-Jose, M. W. de Moor, A. Geresdi, E. J. Lee, J. Klinovaja, D. Loss, J. Nygård, R. Aguado, and L. P. Kouwenhoven, From Andreev to Majorana bound states in hybrid superconductor–semiconductor nanowires, Nat. Rev. Phys. **2**, 575 (2020).

[6] P. Marra, Majorana nanowires for topological quantum computation, J. Appl. Phys. **132**, 231101 (2022).

[7] A. Y. Kitaev, Unpaired Majorana fermions in quantum wires, Phys. Usp. **44**, 131 (2001).

[8] D. Aasen, M. Hell, R. V. Mishmash, A. Higginbotham, J. Danon, M. Leijnse, T. S. Jespersen, J. A. Folk, C. M. Marcus, K. Flensberg, and J. Alicea, Milestones toward Majorana-based quantum computing, Phys. Rev. X **6**, 031016 (2016).

[9] C. W. J. Beenakker, Search for non-Abelian Majorana braiding statistics in superconductors, SciPost Phys. Lect. Notes **1**, 15 (2020).

[10] S. D. Sarma, M. Freedman, and C. Nayak, Majorana zero modes and topological quantum computation, npj Quantum Inf. **1**, 15001 (2015).

[11] K. Flensberg, F. von Oppen, and A. Stern, Engineered platforms for topological superconductivity and Majorana zero modes, Nat. Rev. Mater. **6**, 944 (2021).

[12] H. Zhang, D. E. Liu, M. Wimmer, and L. P. Kouwenhoven, Next steps of quantum transport in Majorana nanowire devices, Nat. Commun. **10**, 5128 (2019).

[13] L. Fu and C. L. Kane, Superconducting proximity effect and Majorana fermions at the surface of a topological insulator, Phys. Rev. Lett. **100**, 096407 (2008).

[14] E. Bocquillon, R. S. Deacon, J. Wiedenmann, P. Leubner, T. M. Klapwijk, C. Brüne, K. Ishibashi, H. Buhmann, and L. W. Molenkamp, Gapless Andreev bound states in the quantum spin Hall insulator HgTe, Nat. Nanotechnol. **12**, 137 (2017).

[15] Y. Oreg, G. Refael, and F. von Oppen, Helical liquids and Majorana bound states in quantum wires, Phys. Rev. Lett. **105**, 177002 (2010).

[16] R. M. Lutchyn, J. D. Sau, and S. Das Sarma, Majorana fermions and a topological phase transition in semiconductor-superconductor heterostructures, Phys. Rev. Lett. **105**, 077001 (2010).

[17] V. Mourik, K. Zuo, S. M. Frolov, S. R. Plissard, E. P. A. M. Bakkers, and L. P. Kouwenhoven, Signatures of Majorana fermions in hybrid superconductor-semiconductor nanowire devices, Science **336**, 1003 (2012).

[18] F. Pientka, A. Keselman, E. Berg, A. Yacoby, A. Stern, and B. I. Halperin, Topological superconductivity in a planar Josephson junction, Phys. Rev. X **7**, 021032 (2017).

[19] M. Hell, M. Leijnse, and K. Flensberg, Two-dimensional platform for networks of Majorana bound states, Phys. Rev. Lett. **118**, 107701 (2017).

[20] A. Fornieri, A. M. Whiticar, F. Setiawan, E. Portolés, A. C. C. Drachmann, A. Keselman, S. Gronin, C. Thomas, T. Wang, R. Kallaher, G. C. Gardner, E. Berg, M. J. Manfra, A. Stern, C. M. Marcus, and F. Nichele, Evidence of topological superconductivity in planar Josephson junctions, Nature (London) **569**, 89 (2019).

[21] H. Ren, F. Pientka, S. Hart, A. T. Pierce, M. Kosowsky, L. Lunczer, R. Schlereth, B. Scharf, E. M. Hankiewicz, L. W. Molenkamp, B. I. Halperin, and A. Yacoby, Topological super-

conductivity in a phase-controlled Josephson junction, Nature (London) **569**, 93 (2019).

[22] T. Laeven, B. Nijholt, M. Wimmer, and A. R. Akhmerov, Enhanced proximity effect in zigzag-shaped Majorana Josephson junctions, Phys. Rev. Lett. **125**, 086802 (2020).

[23] P. P. Paudel, T. Cole, B. D. Woods, and T. D. Stanescu, Enhanced topological superconductivity in spatially modulated planar Josephson junctions, Phys. Rev. B **104**, 155428 (2021).

[24] D. Kuiri and M. P. Nowak, Nonlocal transport signatures of topological superconductivity in a phase-biased planar Josephson junction, Phys. Rev. B **108**, 205405 (2023).

[25] S. Nadj-Perge, I. K. Drozdov, B. A. Bernevig, and A. Yazdani, Proposal for realizing Majorana fermions in chains of magnetic atoms on a superconductor, Phys. Rev. B **88**, 020407(R) (2013).

[26] F. Pientka, L. I. Glazman, and F. von Oppen, Topological superconducting phase in helical Shiba chains, Phys. Rev. B **88**, 155420 (2013).

[27] S. Nadj-Perge, I. K. Drozdov, J. Li, H. Chen, S. Jeon, J. Seo, A. H. MacDonald, B. A. Bernevig, and A. Yazdani, Observation of Majorana fermions in ferromagnetic atomic chains on a superconductor, Science **346**, 602 (2014).

[28] J. D. Sau, R. M. Lutchyn, S. Tewari, and S. Das Sarma, Generic new platform for topological quantum computation using semiconductor heterostructures, Phys. Rev. Lett. **104**, 040502 (2010).

[29] S. Manna, P. Wei, Y. Xie, K. T. Law, P. A. Lee, and J. S. Moodera, Signature of a pair of Majorana zero modes in superconducting gold surface states, Proc. Natl. Acad. Sci. **117**, 8775 (2020).

[30] A. Maiani, R. S. Souto, M. Leijnse, and K. Flensberg, Topological superconductivity in semiconductor–superconductor–magnetic-insulator heterostructures, Phys. Rev. B **103**, 104508 (2021).

[31] S. D. Escribano, E. Prada, Y. Oreg, and A. L. Yeyati, Tunable proximity effects and topological superconductivity in ferromagnetic hybrid nanowires, Phys. Rev. B **104**, L041404 (2021).

[32] C.-X. Liu, S. Schuwalow, Y. Liu, K. Vilkelis, A. L. R. Manesco, P. Krogstrup, and M. Wimmer, Electronic properties of InAs/EuS/Al hybrid nanowires, Phys. Rev. B **104**, 014516 (2021).

[33] B. D. Woods and T. D. Stanescu, Electrostatic effects and topological superconductivity in semiconductor–superconductor–magnetic-insulator hybrid wires, Phys. Rev. B **104**, 195433 (2021).

[34] A. Khindanov, J. Alicea, P. Lee, W. S. Cole, and A. E. Antipov, Topological superconductivity in nanowires proximate to a diffusive superconductor–magnetic-insulator bilayer, Phys. Rev. B **103**, 134506 (2021).

[35] J. Langbehn, S. A. González, P. W. Brouwer, and F. von Oppen, Topological superconductivity in tripartite superconductor-ferromagnet-semiconductor nanowires, Phys. Rev. B **103**, 165301 (2021).

[36] K. Pöyhönen, D. Varjas, M. Wimmer, and A. R. Akhmerov, Minimal Zeeman field requirement for a topological transition in superconductors, SciPost Phys. **10**, 108 (2021).

[37] M. C. Dartiailh, W. Mayer, J. Yuan, K. S. Wickramasinghe, A. Matos-Abiague, I. Žutić, and J. Shabani, Phase signature of

topological transition in Josephson junctions, Phys. Rev. Lett. **126**, 036802 (2021).

[38] S. Vaitiekėnas, Y. Liu, P. Krogstrup, and C. Marcus, Zero-bias peaks at zero magnetic field in ferromagnetic hybrid nanowires, Nat. Phys. **17**, 43 (2021).

[39] S. D. Escribano, A. Maiani, M. Leijnse, K. Flensberg, Y. Oreg, A. Levy Yeyati, E. Prada, and R. Seoane Souto, Semiconductor-ferromagnet-superconductor planar heterostructures for 1D topological superconductivity, npj Quantum Mater. **7**, 81 (2022).

[40] S. Vaitiekėnas, R. S. Souto, Y. Liu, P. Krogstrup, K. Flensberg, M. Leijnse, and C. M. Marcus, Evidence for spin-polarized bound states in semiconductor–superconductor–ferromagnetic-insulator islands, Phys. Rev. B **105**, L041304 (2022).

[41] D. Razmadze, R. S. Souto, L. Galletti, A. Maiani, Y. Liu, P. Krogstrup, C. Schrade, A. Gyenis, C. M. Marcus, and S. Vaitiekėnas, Supercurrent reversal in ferromagnetic hybrid nanowire Josephson junctions, Phys. Rev. B **107**, L081301 (2023).

[42] M. M. Desjardins, L. C. Contamin, M. R. Delbecq, M. C. Dartiailh, L. E. Bruhat, T. Cubaynes, J. J. Viennot, F. Mallet, S. Rohart, A. Thiaville, A. Cottet, and T. Kontos, Synthetic spin–orbit interaction for Majorana devices, Nat. Mater. **18**, 1060 (2019).

[43] A. Yazdani, Conjuring Majorana with synthetic magnetism, Nat. Mater. **18**, 1036 (2019).

[44] R. Egger and K. Flensberg, Emerging Dirac and Majorana fermions for carbon nanotubes with proximity-induced pairing and spiral magnetic field, Phys. Rev. B **85**, 235462 (2012).

[45] O. Lesser, G. Shavit, and Y. Oreg, Topological superconductivity in carbon nanotubes with a small magnetic flux, Phys. Rev. Res. **2**, 023254 (2020).

[46] D. Steffensen, M. H. Christensen, B. M. Andersen, and P. Kotetes, Topological superconductivity induced by magnetic texture crystals, Phys. Rev. Res. **4**, 013225 (2022).

[47] B. Braunecker, G. I. Japaridze, J. Klinovaja, and D. Loss, Spin-selective Peierls transition in interacting one-dimensional conductors with spin-orbit interaction, Phys. Rev. B **82**, 045127 (2010).

[48] B. Braunecker and P. Simon, Interplay between classical magnetic moments and superconductivity in quantum one-dimensional conductors: Toward a self-sustained topological Majorana phase, Phys. Rev. Lett. **111**, 147202 (2013).

[49] J. Klinovaja, P. Stano, A. Yazdani, and D. Loss, Topological superconductivity and Majorana fermions in RKKY systems, Phys. Rev. Lett. **111**, 186805 (2013).

[50] T.-P. Choy, J. M. Edge, A. R. Akhmerov, and C. W. J. Beenakker, Majorana fermions emerging from magnetic nanoparticles on a superconductor without spin-orbit coupling, Phys. Rev. B **84**, 195442 (2011).

[51] M. M. Vazifeh and M. Franz, Self-organized topological state with Majorana fermions, Phys. Rev. Lett. **111**, 206802 (2013).

[52] K. Pöyhönen, A. Weststrom, J. Röntynen, and T. Ojanen, Majorana states in helical Shiba chains and ladders, Phys. Rev. B **89**, 115109 (2014).

[53] A. Heimes, P. Kotetes, and G. Schön, Majorana fermions from Shiba states in an antiferromagnetic chain on top of a superconductor, Phys. Rev. B **90**, 060507(R) (2014).

[54] J. Xiao and J. An, Chiral symmetries and Majorana fermions in coupled magnetic atomic chains on a superconductor, New J. Phys. **17**, 113034 (2015).

[55] M. Schecter, K. Flensberg, M. H. Christensen, B. M. Andersen, and J. Paaske, Self-organized topological superconductivity in a Yu-Shiba-Rusinov chain, Phys. Rev. B **93**, 140503(R) (2016).

[56] M. H. Christensen, M. Schecter, K. Flensberg, B. M. Andersen, and J. Paaske, Spiral magnetic order and topological superconductivity in a chain of magnetic adatoms on a two-dimensional superconductor, Phys. Rev. B **94**, 144509 (2016).

[57] P. Marra and M. Cuoco, Controlling Majorana states in topologically inhomogeneous superconductors, Phys. Rev. B **95**, 140504(R) (2017).

[58] H. Kim, A. Palacio-Morales, T. Posske, L. Rózsa, K. Palotás, L. Szunyogh, M. Thorwart, and R. Wiesendanger, Toward tailoring Majorana bound states in artificially constructed magnetic atom chains on elemental superconductors, Sci. Adv. **4**, aar5251 (2018).

[59] D. Mondal, A. K. Ghosh, T. Nag, and A. Saha, Engineering anomalous Floquet Majorana modes and their time evolution in a helical Shiba chain, Phys. Rev. B **108**, L081403 (2023).

[60] M. Kjaergaard, K. Wölms, and K. Flensberg, Majorana fermions in superconducting nanowires without spin-orbit coupling, Phys. Rev. B **85**, 020503(R) (2012).

[61] J. Klinovaja, P. Stano, and D. Loss, Transition from fractional to Majorana fermions in Rashba nanowires, Phys. Rev. Lett. **109**, 236801 (2012).

[62] J. Klinovaja and D. Loss, Giant spin-orbit interaction due to rotating magnetic fields in graphene nanoribbons, Phys. Rev. X **3**, 011008 (2013).

[63] V. Kornich, M. G. Vavilov, M. Friesen, M. A. Eriksson, and S. N. Coppersmith, Majorana bound states in nanowire-superconductor hybrid systems in periodic magnetic fields, Phys. Rev. B **101**, 125414 (2020).

[64] M. J. A. Jardine, J. P. T. Stenger, Y. Jiang, E. J. de Jong, W. Wang, A. C. B. Jayich, and S. M. Frolov, Integrating micromagnets and hybrid nanowires for topological quantum computing, SciPost Phys. **11**, 090 (2021).

[65] S. Nakosai, Y. Tanaka, and N. Nagaosa, Two-dimensional *p*-wave superconducting states with magnetic moments on a conventional *s*-wave superconductor, Phys. Rev. B **88**, 180503(R) (2013).

[66] W. Chen and A. P. Schnyder, Majorana edge states in superconductor-noncollinear magnet interfaces, Phys. Rev. B **92**, 214502 (2015).

[67] N. Sedlmayr, J. M. Aguiar-Hualde, and C. Bena, Flat Majorana bands in two-dimensional lattices with inhomogeneous magnetic fields: Topology and stability, Phys. Rev. B **91**, 115415 (2015).

[68] G. L. Fatin, A. Matos-Abiague, B. Scharf, and I. Žutić, Wireless Majorana bound states: From magnetic tunability to braiding, Phys. Rev. Lett. **117**, 077002 (2016).

[69] P. Virtanen, F. S. Bergeret, E. Strambini, F. Giazotto, and A. Braggio, Majorana bound states in hybrid two-dimensional Josephson junctions with ferromagnetic insulators, Phys. Rev. B **98**, 020501(R) (2018).

[70] G. Livanas, M. Sigrist, and G. Varelogiannis, Alternative paths to realize Majorana fermions in superconductor-ferromagnet heterostructures, Sci. Rep. **9**, 6259 (2019).

[71] N. Mohanta, T. Zhou, J.-W. Xu, J. E. Han, A. D. Kent, J. Shabani, I. Žutić, and A. Matos-Abiague, Electrical control of Majorana bound states using magnetic stripes, Phys. Rev. Appl. **12**, 034048 (2019).

[72] T. Zhou, N. Mohanta, J. E. Han, A. Matos-Abiague, and I. Žutić, Tunable magnetic textures in spin valves: From spintronics to Majorana bound states, Phys. Rev. B **99**, 134505 (2019).

[73] J. Bedow, E. Mascot, T. Posske, G. S. Uhrig, R. Wiesendanger, S. Rachel, and D. K. Morr, Topological superconductivity induced by a triple-q magnetic structure, Phys. Rev. B **102**, 180504(R) (2020).

[74] C. Xiao, J. Tang, P. Zhao, Q. Tong, and W. Yao, Chiral channel network from magnetization textures in two-dimensional MnBi$_2$Te$_4$, Phys. Rev. B **102**, 125409 (2020).

[75] S. Turcotte, S. Boutin, J. C. Lemyre, I. Garate, and M. Pioro-Ladrière, Optimized micromagnet geometries for Majorana zero modes in low *g*-factor materials, Phys. Rev. B **102**, 125425 (2020).

[76] D. Steffensen, B. M. Andersen, and P. Kotetes, Trapping Majorana zero modes in vortices of magnetic texture crystals coupled to nodal superconductors, Phys. Rev. B **104**, 174502 (2021).

[77] G. Livanas, N. Vanas, and G. Varelogiannis, Majorana zero modes in ferromagnetic wires without spin-orbit coupling, Condens. Matter **6**, 6040044 (2021).

[78] G. Livanas, N. Vanas, M. Sigrist *et al.*, Platform for controllable Majorana zero modes using superconductor/ferromagnet heterostructures, Eur. Phys. J. B **95**, 47 (2022).

[79] P. Chatterjee, A. K. Ghosh, A. K. Nandy, and A. Saha, Second-order topological superconductor via noncollinear magnetic texture, Phys. Rev. B **109**, L041409 (2024).

[80] K. Pöyhönen, A. Weststrom, S. S. Pershoguba, T. Ojanen, and A. V. Balatsky, Skyrmion-induced bound states in a *p*-wave superconductor, Phys. Rev. B **94**, 214509 (2016).

[81] E. Mascot, J. Bedow, M. Graham, S. Rachel, and D. K. Morr, Topological superconductivity in skyrmion lattices, npj Quantum Mater. **6**, 6 (2021).

[82] N. Mohanta, S. Okamoto, and E. Dagotto, Skyrmion control of Majorana states in planar Josephson junctions, Commun. Phys. **4**, 163 (2021).

[83] S. A. Díaz, J. Klinovaja, D. Loss, and S. Hoffman, Majorana bound states induced by antiferromagnetic skyrmion textures, Phys. Rev. B **104**, 214501 (2021).

[84] A. Kubetzka, J. M. Bürger, R. Wiesendanger, and K. von Bergmann, Towards skyrmion-superconductor hybrid systems, Phys. Rev. Mater. **4**, 081401(R) (2020).

[85] A. P. Petrović, M. Raju, X. Y. Tee, A. Louat, I. Maggio-Aprile, R. M. Menezes, M. J. Wyszyński, N. K. Duong, M. Reznikov, C. Renner, M. V. Milošević, and C. Panagopoulos, Skyrmion-(anti)vortex coupling in a chiral magnet-superconductor heterostructure, Phys. Rev. Lett. **126**, 117205 (2021).

[86] A. Palacio-Morales, E. Mascot, S. Cocklin, H. Kim, S. Rachel, D. K. Morr, and R. Wiesendanger, Atomic-scale interface engineering of Majorana edge modes in a 2D magnet-superconductor hybrid system, Sci. Adv. **5**, eaav6600 (2019).

[87] G. C. Ménard, A. Mesaros, C. Brun, F. Debontridder, D. Roditchev, P. Simon, and T. Cren, Isolated pairs of Majorana zero modes in a disordered superconducting lead monolayer, Nat. Commun. **10**, 2587 (2019).

[88] S. Kezilebieke, M. N. Huda, V. Vaňo, M. Aapro, S. C. Ganguli, O. J. Silveira, S. Głodzik, A. S. Foster, T. Ojanen, and P. Liljeroth, Topological superconductivity in a van der Waals heterostructure, Nature (London) **588**, 424 (2020).

[89] O. Lesser and Y. Oreg, Majorana zero modes induced by superconducting phase bias, J. Phys. D **55**, 164001 (2022).

[90] C. T. Ke, C. M. Moehle, F. K. de Vries, C. Thomas, S. Metti, C. R. Guinn, R. Kallaher, M. Lodari, G. Scappucci, T. Wang, R. E. Diaz, G. C. Gardner, M. J. Manfra, and S. Goswami, Ballistic superconductivity and tunable π–junctions in InSb quantum wells, Nat. Commun. **10**, 3764 (2019).

[91] A. Banerjee, M. Geier, M. A. Rahman, D. S. Sanchez, C. Thomas, T. Wang, M. J. Manfra, K. Flensberg, and C. M. Marcus, Control of Andreev bound states using superconducting phase texture, Phys. Rev. Lett. **130**, 116203 (2023).

[92] A. Banerjee, O. Lesser, M. A. Rahman, H.-R. Wang, M.-R. Li, A. Kringhøj, A. M. Whiticar, A. C. C. Drachmann, C. Thomas, T. Wang, M. J. Manfra, E. Berg, Y. Oreg, A. Stern, and C. M. Marcus, Signatures of a topological phase transition in a planar Josephson junction, Phys. Rev. B **107**, 245304 (2023).

[93] V. K. Dugaev, V. R. Vieira, P. D. Sacramento, J. Barnaś, M. A. N. Araújo, and J. Berakdar, Current-induced spin torque on a domain wall in a magnetic nanowire, Int. J. Mod. Phys. B **21**, 1659 (2007).

[94] T. Mizushima and M. Sato, Topological phases of quasi-one-dimensional fermionic atoms with a synthetic gauge field, New J. Phys. **15**, 075010 (2013).

[95] I. C. Fulga, F. Hassler, and A. R. Akhmerov, Scattering theory of topological insulators and superconductors, Phys. Rev. B **85**, 165409 (2012).

[96] See Supplemental Material at http://link.aps.org/supplemental/10.1103/PhysRevB.110.L060505 for a description of the one-dimensional model, the domain magnetic texture, the approximate topological invariant for finite-size systems, and the role of disorder and band filling, which includes Refs. [94,95,120–124].

[97] C. W. J. Beenakker and H. van Houten, Josephson current through a superconducting quantum point contact shorter than the coherence length, Phys. Rev. Lett. **66**, 3056 (1991).

[98] F. S. Bergeret, A. F. Volkov, and K. B. Efetov, Odd triplet superconductivity and related phenomena in superconductor-ferromagnet structures, Rev. Mod. Phys. **77**, 1321 (2005).

[99] T. Tokuyasu, J. A. Sauls, and D. Rainer, Proximity effect of a ferromagnetic insulator in contact with a superconductor, Phys. Rev. B **38**, 8823 (1988).

[100] M. Haze, Y. Yoshida, and Y. Hasegawa, Experimental verification of the rotational type of chiral spin spiral structures by spin-polarized scanning tunneling microscopy, Sci. Rep. **7**, 13269 (2017).

[101] M. J. Meijer, J. Lucassen, R. A. Duine, H. J. M. Swagten, B. Koopmans, R. Lavrijsen, and M. H. D. Guimarães, Chiral spin spirals at the surface of the van der Waals ferromagnet Fe$_3$GeTe$_2$, Nano Lett. **20**, 8563 (2020).

[102] L. Peng, F. S. Yasin, T.-E. Park, S. J. Kim, X. Zhang, T. Nagai, K. Kimoto, S. Woo, and X. Yu, Tunable Néel–Bloch magnetic

twists in Fe_3GeTe_2 with van der Waals structure, Adv. Funct. Mater. **31**, 2103583 (2021).

[103] Y. Gao, X. Zheng, Z. Li, J. Xu, J. Qi, Y. Guo, C. Hu, W. Qin, C. He, S. Shen, H. Wei, Y. Zhang, and S. Wang, Real-space observation of non-collinear spin structure in centrosymmetric TbGa rare-earth magnet, AIP Adv. **12**, 055315 (2022).

[104] R. Abd-Shukor, Coherence length versus transition temperature of hydride-based and room temperature superconductors, Results Phys. **25**, 104219 (2021).

[105] A. Peri, I. Mangel, and A. Keren, Superconducting stiffness and coherence length of $FeSe_{0.5}Te_{0.5}$ measured in a zero-applied field, Condens. Matter **8**, 39 (2023).

[106] A. Maiani, A. C. C. Drachmann, L. Galletti, C. Schrade, Y. Liu, R. S. Souto, and S. Vaitiekėnas, Percolative supercurrent in superconductor-ferromagnetic insulator bilayers, arXiv:2404.17320.

[107] D.-L. Bao, A. O'Hara, S. Du, and S. T. Pantelides, Tunable, ferroelectricity-inducing, spin-spiral magnetic ordering in monolayer FeOCl, Nano Lett. **22**, 3598 (2022).

[108] N. Yabuki, R. Moriya, M. Arai, Y. Sata, S. Morikawa, S. Masubuchi, and T. Machida, Supercurrent in van der Waals Josephson junction, Nat. Commun. **7**, 10616 (2016).

[109] M. Kim, G.-H. Park, J. Lee, J. H. Lee, J. Park, H. Lee, G.-H. Lee, and H.-J. Lee, Strong proximity Josephson coupling in vertically stacked $NbSe_2$–graphene–$NbSe_2$ van der Waals junctions, Nano Lett. **17**, 6125 (2017).

[110] T. Dvir, A. Zalic, E. H. Fyhn, M. Amundsen, T. Taniguchi, K. Watanabe, J. Linder, and H. Steinberg, Planar graphene-nbse$_2$ Josephson junctions in a parallel magnetic field, Phys. Rev. B **103**, 115401 (2021).

[111] H. Idzuchi, F. Pientka, K.-F. Huang, K. Harada, Ö. Gül, Y. J. Shin, L. T. Nguyen, N. H. Jo, D. Shindo, R. J. Cava, P. C. Canfield, and P. Kim, Unconventional supercurrent phase in Ising superconductor Josephson junction with atomically thin magnetic insulator, Nat. Commun. **12**, 5332 (2021).

[112] L. Ai, E. Zhang, J. Yang, X. Xie, Y. Yang, Z. Jia, Y. Zhang, S. Liu, Z. Li, P. Leng, X. Cao, X. Sun, T. Zhang, X. Kou, Z. Han, F. Xiu, and S. Dong, Van der Waals ferromagnetic Josephson junctions, Nat. Commun. **12**, 6580 (2021).

[113] C. Bell, E. J. Tarte, G. Burnell, C. W. Leung, D.-J. Kang, and M. G. Blamire, Proximity and Josephson effects in superconductor/antiferromagnetic $Nb/\gamma - Fe_{50}Mn_{50}$ heterostructures, Phys. Rev. B **68**, 144517 (2003); **69**, 109903(E) (2004).

[114] A. Kamra, A. Rezaei, and W. Belzig, Spin splitting induced in a superconductor by an antiferromagnetic insulator, Phys. Rev. Lett. **121**, 247702 (2018).

[115] J. L. Lado and M. Sigrist, Two-dimensional topological superconductivity with antiferromagnetic insulators, Phys. Rev. Lett. **121**, 037002 (2018).

[116] S. S. Luntama, P. Törmä, and J. L. Lado, Interaction-induced topological superconductivity in antiferromagnet-superconductor junctions, Phys. Rev. Res. **3**, L012021 (2021).

[117] E. H. Fyhn, A. Brataas, A. Qaiumzadeh, and J. Linder, Superconducting proximity effect and long-ranged triplets in dirty metallic antiferromagnets, Phys. Rev. Lett. **131**, 076001 (2023).

[118] S. Chourasia, L. J. Kamra, I. V. Bobkova, and A. Kamra, Generation of spin-triplet Cooper pairs via a canted antiferromagnet, Phys. Rev. B **108**, 064515 (2023).

[119] L. J. Kamra, S. Chourasia, G. A. Bobkov, V. M. Gordeeva, I. V. Bobkova, and A. Kamra, Complete T_c suppression and Néel triplets mediated exchange in antiferromagnet-superconductor-antiferromagnet trilayers, Phys. Rev. B **108**, 144506 (2023).

[120] A. P. Schnyder, S. Ryu, A. Furusaki, and A. W. W. Ludwig, Classification of topological insulators and superconductors in three spatial dimensions, Phys. Rev. B **78**, 195125 (2008).

[121] S. Tewari and J. D. Sau, Topological invariants for spin-orbit coupled superconductor nanowires, Phys. Rev. Lett. **109**, 150408 (2012).

[122] A. Altland and M. R. Zirnbauer, Nonstandard symmetry classes in mesoscopic normal-superconducting hybrid structures, Phys. Rev. B **55**, 1142 (1997).

[123] J. Cayao and P. Burset, Confinement-induced zero-bias peaks in conventional superconductor hybrids, Phys. Rev. B **104**, 134507 (2021).

[124] A. M. Zagoskin, *Quantum Theory of Many-Body Systems* (Springer, Berlin, 1998), Vol. 174.